

# Context-specific interactions between Notch and ALK1 cannot explain ALK1-associated arteriovenous malformations

Elizabeth R. Rochon<sup>1</sup>, Daniel S. Wright<sup>1†</sup>, Max M. Schubert<sup>1</sup>, and Beth L. Roman<sup>1,2\*</sup>

<sup>1</sup>Department of Biological Sciences, University of Pittsburgh, Pittsburgh, PA 15260, USA; and <sup>2</sup>Department of Human Genetics, University of Pittsburgh Graduate School of Public Health, 130 DeSoto St, Pittsburgh, PA 15261, USA

Received 10 November 2014; revised 24 April 2015; accepted 7 May 2015; online publish-ahead-of-print 12 May 2015

Time for primary review: 55 days

## Aims

Notch and activin receptor-like kinase 1 (ALK1) have been implicated in arterial specification, angiogenic tip/stalk cell differentiation, and development of arteriovenous malformations (AVMs), and ALK1 can cooperate with Notch to up-regulate expression of Notch target genes in cultured endothelial cells. These findings suggest that Notch and ALK1 might collaboratively program arterial identity and prevent AVMs. We therefore sought to investigate the interaction between Notch and Alk1 signalling in the developing vertebrate vasculature.

## Methods and results

We modulated Notch and Alk1 activities in zebrafish embryos and examined effects on Notch target gene expression and vascular morphology. Although Alk1 is not necessary for expression of Notch target genes in arterial endothelium, loss of Notch signalling unmasks a role for Alk1 in supporting *hey2* and *ephrinb2a* expression in the dorsal aorta. In contrast, Notch and Alk1 play opposing roles in *hey2* expression in cranial arteries and *dll4* expression in all arterial endothelium, with Notch inducing and Alk1 repressing these genes. Although *alk1* loss increases expression of *dll4*, AVMs in *alk1* mutants could neither be phenocopied by Notch activation nor rescued by Dll4/Notch inhibition.

## Conclusion

Control of Notch targets in arterial endothelium is context-dependent, with gene-specific and region-specific requirements for Notch and Alk1. Alk1 is not required for arterial identity, and perturbations in Notch signalling cannot account for *alk1* mutant-associated AVMs. These data suggest that AVMs associated with ALK1 mutation are not caused by defective arterial specification or altered Notch signalling.

## Keywords

Activin receptor-like kinase 1 • Notch • Arteriovenous malformation • Zebrafish • Angiogenesis

## 1. Introduction

When activated by transmembrane ligands of the Delta and Jagged families, the Notch intracellular domain (NICD) is cleaved, translocates to the nucleus, binds to the DNA binding protein, recombination signal binding protein for immunoglobulin kappa J (RBPJ), and induces target gene expression.<sup>1</sup> In the vasculature, delta-like ligand 4 (Dll4)/Notch signalling controls arterial specification and angiogenic tip/stalk cell selection,<sup>2–5</sup> and in mouse and zebrafish models, decreased Dll4/Notch function leads to direct connections between arteries and veins, or arteriovenous malformations (AVMs).<sup>2,6–9</sup> Because Dll4/Notch signalling transcriptionally up-regulates the arterial endothelial marker, *ephrinb2* (*Efnb2*),<sup>10</sup> and decreased Dll4/Notch signalling results in loss of *Efnb2*

and ectopic arterial expression of the venous marker, *Ephb4*,<sup>2,6–8,10–13</sup> AVMs resulting from decreased Dll4/Notch signalling are generally attributed to disruption of arterial-venous identity. Notch loss-of-function (Notch<sup>lof</sup>) generates small calibre AVMs that are associated with thin, nearly atretic arteries.<sup>6,7,14</sup> Notch gain-of-function (Notch<sup>gof</sup>), which enhances *Efnb2* and represses *Ephb4*, also results in AVMs in mice.<sup>2,6–8,10–13</sup> and human brain AVMs exhibit increased Notch signalling.<sup>15,16</sup> AVMs associated with Notch<sup>gof</sup> involve enlarged arteries containing supernumerary endothelial cells,<sup>8,9,11,12,17</sup> suggesting that failed repulsion mediated by EfnB2/EphB4, which is required for segregation of venous and arterial cells in developing vessels,<sup>18,19</sup> may be responsible for these AVMs. Thus, both Notch<sup>lof</sup> and Notch<sup>gof</sup> result in AVMs associated with disrupted arterial-venous identity, but the morphological

\* Corresponding author: Tel: +1 412 624 7006; Email: romanb@pitt.edu

† Present address: Behavioural Biology, Center for Behaviour and Neurosciences, University of Groningen, Groningen, The Netherlands.

characteristics of these AVMs are distinct, with low flow, small calibre shunts associated with Notch<sup>lof</sup> and high flow, large calibre shunts associated with Notch<sup>gof</sup>.

Similar to Notch signalling, bone morphogenetic protein (BMP) signalling has also been implicated in AVM prevention. BMP ligands bind to a heterotetrameric complex of type I and type II serine/threonine kinase receptors; non-signalling type III receptors facilitate ligand binding. Upon complex formation, type II receptors phosphorylate type I receptors, which in turn phosphorylate Smad1, Smad5, and Smad9. Phosphorylated Smads bind to Smad4, translocate to the nucleus, and bind to DNA to regulate gene expression.<sup>20</sup> In humans, heterozygous loss of endoglin (*ENG*, encoding a type III receptor), activin receptor-like kinase 1 (*ACVRL1* or *ALK1*, encoding a type I receptor), or *SMAD4* results in hereditary haemorrhagic telangiectasia (HHT), a disease characterized by a predisposition to development of telangiectasias and AVMs.<sup>21–24</sup> *Alk1* mutant mice exhibit decreased *Efnb2* expression in the dorsal aorta (DA),<sup>25</sup> and BMP9/ALK1 transcriptionally induces *EFNB2* in cultured human umbilical artery endothelial cells,<sup>13</sup> suggesting that ALK1, similar to Notch, is required for arterial identity. Also like Notch, ALK1 has been implicated in maintenance of stalk cell identity.<sup>26</sup> Thus, ALK1 and Notch might function in a common pathway to control arterial and/or stalk cell identity and prevent AVMs.

Several lines of evidence suggest that Notch and ALK1 interact in endothelial cells. Activation of either DLL4/Notch or BMP9/ALK1 in cultured endothelial cells enhances expression of canonical Notch targets *HEY1*, *HEY2*, and *HES1*,<sup>13,26,27</sup> and simultaneous activation of these pathways synergistically increases expression of *HEY1* and *HEY2*.<sup>26</sup> A less dramatic effect on *HEY2* expression is observed in response to combined stimulation by constitutively active Notch (*NICD*) and *ALK1* (*ALK1<sup>CA</sup>*).<sup>10</sup> Induction of *HEY1* and *HEY2* by BMP9/ALK1 requires *SMAD4* but not *RBPJ*,<sup>26</sup> and BMP9 induces *SMAD1/5* binding to *HEY1*, *HEY2*, and *HES1* promoters in cultured human umbilical vein endothelial cells (HUVECs).<sup>28</sup> These findings suggest that BMP9/ALK1 directly stimulates canonical Notch targets by a *SMAD*-dependent and *NICD*/*RBPJ*-independent pathway. Notch and ALK1 additively induce *VEGFR1*, a stalk cell marker, and inhibit *APELIN*, a tip cell marker, and endothelial cells lacking *ALK1*, *SMAD4*, or *HEY2* are more likely to be in the tip position.<sup>26</sup> Together, these results suggest that BMP9/ALK1/*SMAD* signalling induces canonical Notch targets independently of *NICD*/*RBPJ* and reinforces Notch-mediated acquisition of arterial identity and maintenance of stalk cell fate.

Although Notch and ALK1 exhibit synergistic interactions with respect to Notch target gene expression in cultured endothelial cells, evidence for synergy is less compelling for phenotypic endpoints. Both *NICD* and *ALK1<sup>CA</sup>* dampen endothelial cell sprouting, but simultaneous pathway activation shows no further effects, and inhibition of one pathway does not inhibit effects of activation of the other pathway.<sup>13</sup> Similarly, both ALK1 and Notch inhibition enhance VEGF-stimulated tube formation in HUVECs and increase vascular area in the postnatal retina; however, combined inhibition of these pathways shows less than additive effects.<sup>26</sup> Thus, the synergy between Notch and ALK1 in controlling gene expression may not directly translate to synergistic effects on endothelial cell behaviour.

To better understand the interaction between Notch and Alk1, we assayed Notch target gene expression and vascular phenotype in zebrafish embryos with altered Notch and/or Alk1 activity. Results demonstrate that Alk1 is not necessary for maintenance of Notch target genes or arterial identity *in vivo*. However, concomitant inhibition of Notch

and Alk1 revealed context-dependent interactions, with cooperative maintenance of *hey2* and *efnb2a* in the DA but opposing effects on *hey2* and no effect on *efnb2a* in cranial arteries. In addition, we observed increased *dll4* expression in both trunk and cranial arterial endothelium in the absence of Alk1 signalling, in contrast to the loss of expression observed with Notch inhibition. These molecular data suggested that AVMs in *alk1* mutants might arise due to Notch gain-of-function; however, Notch activation failed to phenocopy and Notch inhibition failed to rescue AVMs associated with loss of *alk1*. Taken together, these data demonstrate that Notch and Alk1 exhibit context-specific and target-specific interactions in controlling Notch target gene expression *in vivo*, and that AVMs associated with Alk1 deficiency do not result from perturbations in Notch activity.

## 2. Methods

Additional details can be found in Supplementary material online.

### 2.1 Zebrafish lines and maintenance

All zebrafish (*Danio rerio*) experiments conformed to NIH/NRC guidelines (Guide for the Care and Use of Laboratory Animals) and were approved by the University of Pittsburgh Institutional Animal Care and Use Committee (protocol 12070690690). Animals were maintained according to standard protocols.<sup>29</sup> Mutant lines *alk1<sup>ft09e</sup>* (p.Y88X), *alk1<sup>y6</sup>* (p.L240F), and *alk1<sup>s407</sup>* (g.IVS8-2A>T) are functional nulls and have indistinguishable phenotypes.<sup>30–32</sup> Transgenic lines *Tg(fli1a:GAL4FF)<sup>ubs3</sup>*, *Tg(UAS:Kaede)<sup>rk8</sup>*, *Tg(5xUAS-E1b:6xMYC-notch1a)<sup>kca3</sup>*, *Tg(EPV.TP1-Mmu.Hbb:egfp)<sup>um14</sup>* [abbreviated *Tg(tp1:egfp)<sup>um14</sup>*], *Tg(kdrl:gfp)<sup>at116</sup>*, *Tg(gata1a:dsred)<sup>sd2</sup>* and *Tg(fli1a.ebs:alk1<sup>CA</sup>-mCherry)* have been described.<sup>33–38</sup> *Tg(fli1a.ebs:alk1<sup>CA</sup>-mCherry)* is embryonic lethal; therefore, F1 embryos were analysed from mosaic P0 founders. *Tg(fli1a.ep:mRFP-CAAX)<sup>pt504</sup>*, with mRFP-labelled endothelial cell membranes, was generated using a previously described construct.<sup>31</sup>

### 2.2 Morpholinos and drug treatments

Morpholinos targeting *alk1*<sup>31</sup> and *dll4*<sup>4</sup> have been described and validated; sequences are provided in the Supplementary material online. These morpholinos phenocopy their respective genotypic mutants,<sup>5,31,39,40</sup> supporting the validity of these tools.<sup>41</sup> For Notch inhibition experiments, embryos were exposed to 10 µmol/L LY411575 (Stemgent, Cambridge, MA, USA), 50 µmol/L DAPT (Sigma, St Louis, MO, USA), or 1% dimethyl sulfoxide (DMSO) from 23 to 36 h post-fertilization (hpf) or 23–48 hpf.

### 2.3 In situ hybridization

Whole mount *in situ* hybridization and vibratome sectioning were carried out as described<sup>30,39</sup> using an InSituPro VSi liquid handler (Intavis Inc., Chicago, IL, USA).

### 2.4 Confocal and two-photon imaging and image analysis

Fluorescence imaging was performed using a Leica TCS SP5 multiphoton/confocal microscope (Leica Microsystems, Wetzlar, Germany) as previously described.<sup>39</sup> LAS AF software, version 3.0.0 build 8134, was used to measure fluorescence intensity in *Tg(tp1:egfp)<sup>um14</sup>* embryos. Effects of Notch inhibition and *alk1* mutation on forebrain and midbrain central artery sprouting at 36 hpf were analysed from confocal micrographs using Adobe Photoshop CS6.

### 2.5 Statistical analysis

GraphPad Prism v6.0 was used to analyse data using Student's *t*-test (fluorescence intensities) or one-way ANOVA followed by Tukey's *post-hoc* test (BCA areas, central artery sprouting). Significance was set at  $P < 0.05$ .

### 3. Results

#### 3.1 Notch is active concomitant with Alk1 in cranial arterial endothelium

Because our goal was to determine whether Alk1 and Notch signalling interact during vascular development, and because *alk1* plays a critical role in zebrafish cranial arterial development,<sup>30,31,39</sup> we first assessed Notch activity in cranial endothelium using a double transgenic line, *Tg(tp1:egfp)<sup>um14</sup>;Tg(fli1a.ep:mRFP-CAAX)<sup>pt504</sup>*. These fish report Notch activity, as visualized by EGFP expression,<sup>33</sup> on a background of mRFP-labelled endothelial cells. Embryos were imaged at 36 hpf, a time point when Alk1 is active in cranial arterial endothelium.<sup>39</sup> Notch activity was weak to moderate in cranial arteries, including the first aortic arch (AA1), internal carotid artery (ICA), caudal division of the internal carotid artery (CaDI), optic artery (OA), and basal communicating artery (BCA) (Figure 1A). All of these arteries are *alk1*-positive at 36 hpf.<sup>31</sup> Notch activity was also detected in the *alk1*-negative posterior communicating segments (PCS) and metencephalic arteries (MtA), but was absent in cranial veins (Figure 1A). These data demonstrate that cranial vascular Notch activity is arterial-specific, and that all *alk1*-positive arteries have active Notch signalling.

Next, we assayed cranial vessel expression of endogenous Notch targets. Hairy and enhancer of split (HES)-related proteins are transcriptional repressors that are induced by NICD/RBPJ,<sup>42</sup> and the HES-related genes *HES1*, *HEY1*, and *HEY2* are up-regulated by BMP9/ALK1 in cultured endothelial cells.<sup>10,26,28</sup> The zebrafish genome contains two *hes1* paralogs, *her6* and *her9*.<sup>43</sup> However, neither these genes nor *hey1* were detectable in endothelium at 24–36 hpf (data not shown). In contrast, *hey2* was expressed in all *alk1*-positive cranial arteries at 36 hpf (Figure 1B). *efnb2a*, another Notch target,<sup>10</sup> as well as *dll4*, which encodes a Notch ligand that is positively regulated by Notch signalling,<sup>44–46</sup> were also expressed in all *alk1*-positive cranial arteries at 36 hpf (Figure 1B). *dll4* was additionally expressed in the *alk1*-negative PCS and MtA. These data demonstrate that Notch targets *hey2*, *efnb2a*, and *dll4* are expressed in cranial arterial endothelium concomitant with active Alk1 signalling and are good candidates for cooperative regulation by Notch and Alk1.

#### 3.2 Notch and Alk1 cooperatively regulate *hey2* and *efnb2a* but oppositely regulate *dll4* in the dorsal aorta

To investigate the interaction between Notch and Alk1 in the regulation of Notch targets *in vivo*, we assayed *tp1:egfp*, *hey2*, *efnb2a*, and *dll4* in embryos with impaired Notch and/or Alk1 signalling. To inhibit Notch signalling, we treated embryos with 10  $\mu$ mol/L LY411575, a gamma-secretase inhibitor, between 23 and 36 hpf. This time period brackets the critical time period of Alk1 function: *alk1* is first detectable around 26 hpf, and *alk1* mutation results in enlargement of cranial arteries by 32 hpf.<sup>31</sup> LY411575 treatment had no effect on heartbeat or blood flow but resulted in severe trunk curvature (data not shown) as expected in Notch-inhibited embryos.<sup>2,4,47</sup>

Notch signalling is active in the zebrafish DA throughout embryonic development,<sup>2,5,48</sup> and despite no obvious requirement for Alk1, *alk1* is indeed expressed in the DA as early as 26 hpf.<sup>31</sup> LY411575 treatment resulted in complete loss of DA *tp1:egfp* expression (Figure 2A), demonstrating effective abrogation of NICD/RBPJ-mediated transcription. However, the effect of Notch inhibition on expression of endogenous Notch targets was variable. LY411575 treatment had no effect on *hey2*,

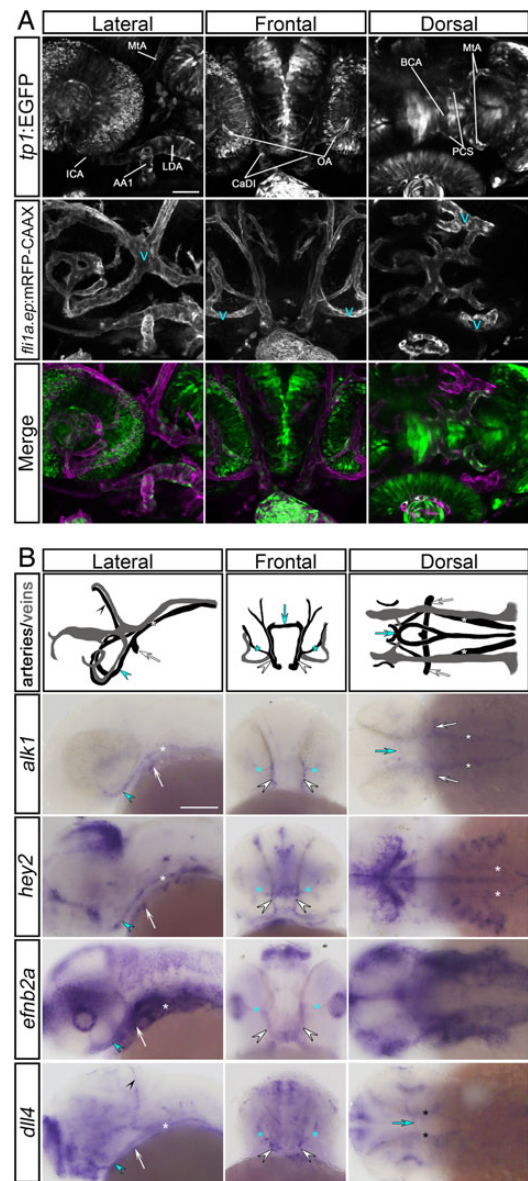


**Figure 1** Notch is active concomitant with Alk1 in cranial arterial endothelium. (A) Notch activity is detectable in cranial arterial but not venous endothelium ('v') at 36 hpf. Two-dimensional confocal projections of *Tg(tp1:egfp)<sup>um14</sup>* (green in merge) and *Tg(fli1a.ep:mRFP-CAAX)<sup>pt504</sup>* (magenta in merge). *alk1*-positive arteries: AA1, aortic arch 1; ICA, internal carotid artery; LDA, lateral dorsal aorta; CaDI, caudal division of internal carotid artery; OA, optic artery; BCA, basal communicating artery. *alk1*-negative arteries: PCS, posterior communicating segment; MtA, metencephalic artery. Images represent  $N = 20$  embryos. Lateral and dorsal views, anterior leftward; frontal view, anterior up. Scale bar, 50  $\mu$ m. (B) Wiring diagrams (arteries black, veins grey) and representative whole mount *in situ* hybridization for *alk1*, *hey2*, *efnb2a*, and *dll4* at 36 hpf. Expression of Notch targets is detected in the *alk1*-positive AA1 (white arrow), ICA (blue arrowhead), LDA (white asterisk), CaDI (white arrowhead), OA (blue asterisk), and BCA (blue arrow). *dll4* is also expressed in the *alk1*-negative PCS (black asterisk) and MtA (black arrowhead). Plane of focus of *dll4*, frontal view, is deeper than other frontal images because of interfering *dll4* brain expression. Images represent  $N > 63$  embryos. Lateral and dorsal views, anterior leftward; frontal view, anterior up. Scale bar, 100  $\mu$ m.



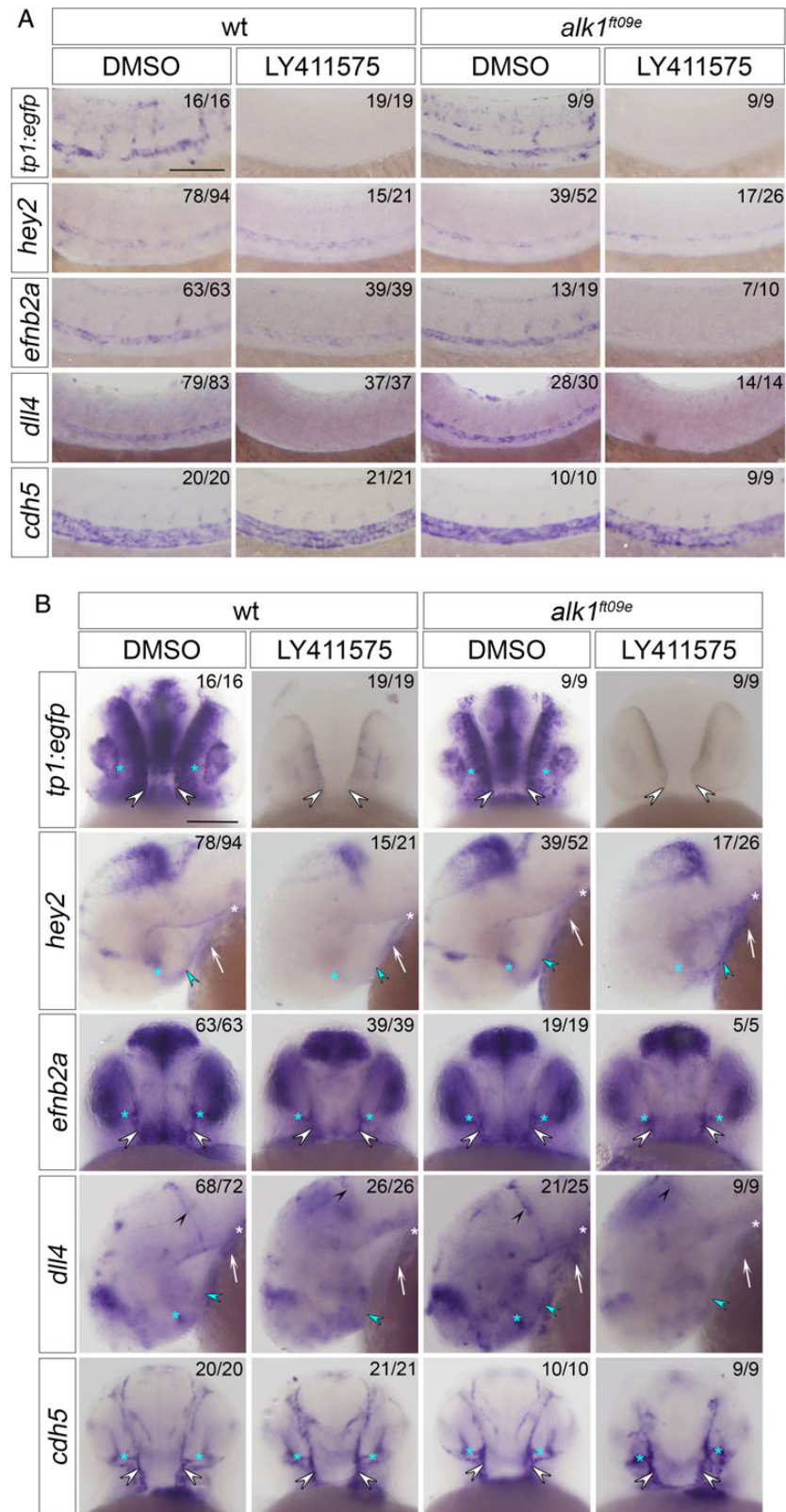


**Figure 2** Notch- and Alk1-mediated control of Notch target gene expression is gene-specific and context-dependent. Whole mount *in situ* hybridization for *tp1:egfp*, *hey2*, *efnb2a*, *dll4*, and *cdh5* in 36 hpf wt and *alk1<sup>ft09e</sup>* embryos treated with 1% DMSO or 10  $\mu$ mol/L LY411575, 23–36 hpf. (A) Trunk. Lateral view, anterior leftwards. (B) Head. AA1, white arrow; ICA, blue arrowhead; LDA, white asterisk; CaDI, white arrowheads; OA, blue asterisks; MtA, black arrowheads. *tp1:egfp*, *efnb2a*, *cdh5*: frontal views, anterior up. *hey2*, *dll4*: lateral views, anterior left. Numbers in upper right corners indicate number of embryos with similar phenotype/total number of embryos assayed. Scale bars, 100  $\mu$ m.

moderately decreased *efnb2a*, and completely abolished *dll4* (Figure 2A). These observations agree with published data<sup>2,40</sup> and suggest that among these DA genes, *dll4* is most sensitive to perturbation of Notch signalling, whereas other pathways maintain *hey2* and *efnb2a* in the absence of Notch.

Next, we examined Notch target gene expression in the DA in *alk1<sup>ft09e</sup>* mutants (Figure 2A). *alk1* mutation had no effect on expression of *tp1:egfp*, *hey2*, or *efnb2a* in the DA (Figure 2A), demonstrating that Alk1 is not necessary for expression of these arterial-specific Notch targets or for acquisition of arterial identity. In contrast, *dll4* expression was up-regulated in the DA in *alk1<sup>ft09e</sup>* mutants (Figure 2A). This observation was confirmed in *alk1<sup>y6</sup>* and *alk1<sup>s407</sup>* mutants and in *alk1* morphants (Supplementary material online, Figure S1A). Furthermore, endothelial-specific expression of *alk1<sup>CA</sup>* (*fli1a.ebs:alk1<sup>CA</sup>-mCherry*) dramatically repressed *dll4* (Supplementary material online, Figure S1B). These data suggest that Alk1 opposes Notch in *dll4* regulation in the DA.

Compared with Notch inhibition alone, combined *alk1<sup>ft09e</sup>* mutation and Notch inhibition had no effect on *tp1:egfp* or *dll4* expression (Figure 2A), supporting the idea that Notch is required for expression of these genes. In contrast, concomitant abrogation of Alk1 and Notch signalling decreased *hey2* and nearly eliminated *efnb2a* (Figure 2A). *hey2* results, originally obtained in LY411575-treated *alk1<sup>ft09e</sup>* embryos, were recapitulated in DAPT-treated *alk1<sup>y6</sup>* mutants and LY411575-treated *alk1* morphants (data not shown). These findings suggest co-operative support of *hey2* and *efnb2a* expression by Notch and Alk1 in the DA and agree with published data suggesting that both genes are regulated independently via NICD/RBPJ and ALK1/Smad1,5.<sup>2,13,26,28</sup>

### 3.3 Notch and Alk1 exhibit gene-specific antagonistic interactions in regulation of cranial arterial endothelial gene expression

We next examined regulation of Notch target genes in cranial arteries, which enlarge upstream of AVMs in *alk1* mutants. LY411575 treatment abrogated *tp1:egfp* expression in cranial arterial endothelium and neural domains (Figure 2B, Supplementary material online, Figure S2), as expected. However, whereas Notch inhibition dramatically decreased *hey2* in cranial arterial endothelium, *efnb2a* was refractory to this treatment (Figure 2B, Supplementary material online, Figure S2). These effects were different from those observed in the DA (Figure 2A), suggesting context-specific gene regulation. LY411575 treatment eliminated arterial *dll4* expression in cranial arteries, similar to the DA, but increased *dll4* in neural tissues (Figure 2B, Supplementary material online, Figure S2). These observations support the idea of a positive

feedback loop specific to arterial endothelial cells in which Notch signalling directly regulates *DLL4* expression.<sup>40,44–46</sup>

As in the DA, in cranial arteries *tp1:egfp*, *hey2*, and *efnb2a* were unaffected by *alk1* mutation or knockdown, whereas *dll4* was markedly up-regulated, and a *fli1a.ebs:alk1<sup>CA</sup>-mCherry* transgene dramatically repressed *dll4* (Figure 2B, Supplementary material online, Figures S1C, D and S2). Also similar to the DA, loss of *alk1* failed to rescue abrogation of *tp1:egfp* or *dll4* expression induced by LY411575 treatment (Figure 2B, Supplementary material online, Figure S2). In contrast, *hey2* and *efnb2a* behaved differently in the absence of both Notch and Alk1 signalling in trunk vs. cranial arterial endothelial domains. In cranial arteries, *efnb2a* expression proved refractory to combined loss of Notch and Alk1 signalling, whereas this same treatment increased *hey2* expression compared with Notch inhibition alone (Figure 2B, Supplementary material online, Figure S2). *hey2* results, originally obtained in LY411575-treated *alk1<sup>ft09e</sup>* embryos, were recapitulated in DAPT-treated *alk1<sup>y6</sup>* mutants and LY411575-treated *alk1* morphants (Supplementary material online, Figure S3). These results suggest that neither Notch nor Alk1 is necessary for cranial arterial *efnb2a* expression, whereas Notch activates and Alk1 dampens *hey2* expression in cranial arteries, with Alk1 acting either downstream of NICD or independently of Notch. These data support the notion that region-specific regulatory networks control arterial expression of Notch target genes. Effects of Notch and Alk1 manipulation on Notch target gene expression are summarized in Table 1.

### 3.4 Notch<sup>gof</sup> and *alk1<sup>lof</sup>* generate vascular morphologies with some phenotypic overlap but with independent aetiologies

Our *in vivo* gene expression studies demonstrated that loss of *alk1* is associated with increased endothelial *dll4* expression. Therefore, we reasoned that enhanced *DLL4*/Notch signalling might phenocopy cranial AVMs in *alk1* mutants. To investigate this possibility, we compared cranial vascular development in wild-type embryos, *Tg(fli1a:GAL4FF)<sup>ubs3</sup>*; *Tg(5xUAS-E1b:6xMYC-notch1a)<sup>kca3</sup>* embryos [which ectopically express Notch1a ICD in all endothelial cells; hereafter referred to as *Tg(endo:N1ICD)*], and *alk1* mutant or morphant embryos.

In wild-type embryos, single sprouts emerged from the most posterior aspect of each bilateral venous primordial midbrain channel (PMBC) ~22 hpf and migrated medially to connect to a sprout emanating from the apex of the paired CaDIs by ~26 hpf, forming the BCA (Supplementary material online, Movie S1). These transient BCA/PMBC connections serve as the primary drainage for the CaDI/BCA between

**Table 1** Qualitative changes in arterial gene expression in response to altered Notch and/or Alk1 signalling<sup>a</sup>

|                 | Dorsal aorta |                             |          | Cranial arteries |                             |          |
|-----------------|--------------|-----------------------------|----------|------------------|-----------------------------|----------|
|                 | Wild-type    | <i>alk1</i> mutant/morphant |          | Wild-type        | <i>alk1</i> mutant/morphant |          |
|                 | LY411575     | DMSO                        | LY411575 | LY411575         | DMSO                        | LY411575 |
| <i>tp1:egfp</i> | ↓↓↓          | NC                          | ↓↓↓      | ↓↓↓              | NC                          | ↓↓↓      |
| <i>hey2</i>     | NC           | NC                          | ↓        | ↓↓               | NC                          | NC       |
| <i>efnb2a</i>   | ↓↓           | NC                          | ↓↓↓      | NC               | NC                          | NC       |
| <i>dll4</i>     | ↓↓↓          | ↑                           | ↓↓↓      | ↓↓↓              | ↑                           | ↓↓↓      |

<sup>a</sup>Embryos were treated with 1% DMSO or 10 μmol/L LY411575, 23–36 hpf, and analysed by *in situ* hybridization at 36 hpf. Table indicates increased (up arrows), decreased (down arrows; number of arrows indicates qualitative strength of response), or no change (NC) in expression compared with DMSO-treated wild-type embryos.



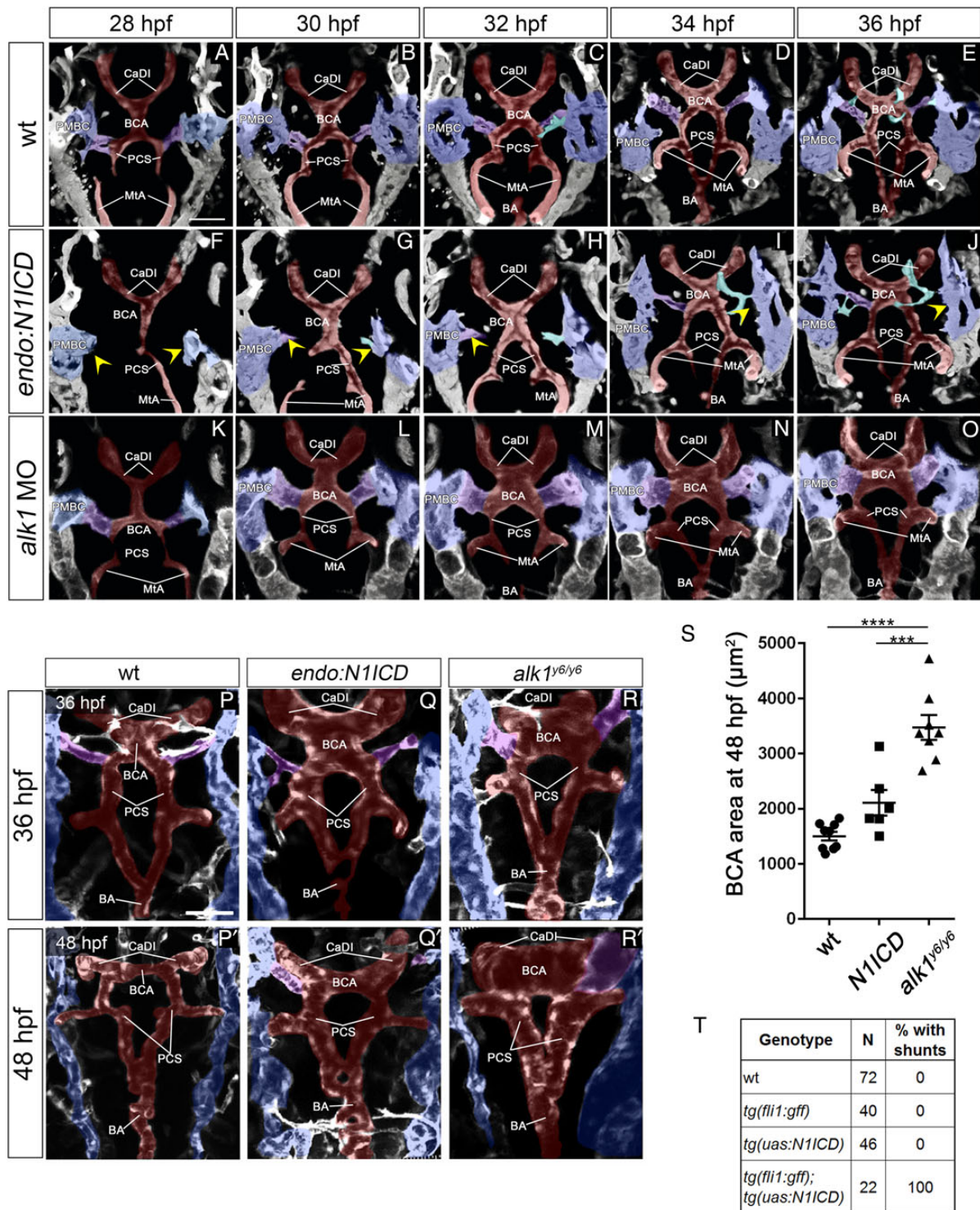


**Figure 3** *notch<sup>gof</sup>* and *alk1<sup>lof</sup>* cranial AVMs have independent aetiologies. (A–J) Cranial arterial development in wt (A–E), *Tg(endo:N1ICD)* (F–J), and *alk1* morphant (K–O) embryos, 28–36 hpf. See also Supplementary material online, *Movies S4–S5*. In *Tg(endo:N1ICD)* embryos (F–J), PMBC-derived sprouts (yellow arrowheads) are delayed, compromising CaDI/BCA drainage. In *alk1* morphant embryos (K–O), connections form normally, but BCA enlargement is evident by 30 hpf. Two-dimensional projections of Z-stacks from two photon/confocal time-lapse imaging, frontal views, anterior up. Images represent  $N = 8$  wt, 6 *Tg(endo:N1ICD)*, 10 *alk1* MO. Endothelial transgenes imaged: wt and *Tg(endo:N1ICD)*, *Tg(fli1a:GAL4FF;UAS:kaede)*; *alk1* MO, *Tg(fli1a:mrfp-caax)<sup>pt504</sup>*. (P–R') Two-photon imaging of wt (P, P'), *Tg(endo:N1ICD)* (Q, Q'), and *alk1<sup>y6/y6</sup>* mutant (R, R') embryos at 36 and 48 hpf. *Tg(endo:N1ICD)* embryos show phenotypic overlap with *alk1* mutants, with variable enlargement of the CaDI (36 hpf) and consistent retention of BCA/PMBC connections (48 hpf). Two-dimensional projections of Z-stacks, dorsal views, anterior up. Images represent  $N = 10$  wt, 8 *Tg(endo:N1ICD)*, and 8 *alk1<sup>y6</sup>*. Imaged transgene is *Tg(kdrl:gfp)<sup>la116</sup>*. (A–R) Pseudocolouring: PMBC (blue), CtA (cyan), CaDI/BCA/PCS/BA (red), BCA/PMBC connection (purple). Scale bars, 50  $\mu\text{m}$ . (S) BCA area at 48 hpf.  $N = 6–9$  for each condition; lines represent mean  $\pm$  SEM. One-way ANOVA followed by Tukey's *post-hoc* test, \*\*\* $P < 0.001$ , \*\*\*\* $P < 0.0001$ . (T) Presence of shunts at 48 hpf.

26 and 36 hpf but regress thereafter as downstream arteries develop (Supplementary material online, *Movie S2*, and Corti *et al.*<sup>31</sup>).

In *Tg(endo:N11CD)* embryos, the CaDIs developed and lumened normally, but sprouting from the PMBC was impaired, with BCA/PMBC connections delayed up to 8 h compared with wild-type [Figure 3, compare A–E, wt to F–J, *Tg(endo:N11CD)*; Supplementary material online, *Movies S3* and *S4*]. Vascular morphology was variable in 36 hpf *Tg(endo:N11CD)* embryos, with establishment of early alternative drainage connections (e.g. BCA to PCS/MtA, Figure 3G and H) associated with relatively normal calibre vessels, and establishment of late connections associated with CaDI/BCA engorgement and enlargement (Figure 3P and Q). Regardless of 36 hpf phenotype, BCA area was not significantly increased compared with control at 48 hpf (Figure 3S), but all *Tg(endo:N11CD)* embryos maintained at least one BCA/PMBC connection, resulting in a small calibre AVM (Figure 3P', Q', T).

Although the *Tg(endo:N11CD)* phenotype bears some resemblance to the *alk1* mutant phenotype, these phenotypes originate and progress differently. In *Tg(endo:N11CD)* embryos, delayed venous sprouting compromises early cranial arterial drainage, resulting in variable changes in CaDI/BCA calibres and small AVMs stemming from persistent BCA/PMBC connections (Figure 3F–J, Q, Q'). In *alk1* morphants or mutants, venous-derived angiogenic sprouting is not delayed, and all vessel connections develop normally (Figure 3K–O; Supplementary material online, *Movie S5*). However, increased endothelial cell number in the CaDI leads to increased calibre and altered haemodynamics, causing

downstream vessels to adapt by maintaining normally transient arterial-venous connections (Figure 3R, R', S), most often between the BCA and PMBC.<sup>30,31,39</sup> Although the *Tg(endo:N11CD)* phenotype decreases in severity over time (Figure 3Q and Q'), the *alk1* mutant phenotype exacerbates over time (Figure 3R and R'), with progressive increases in vessel calibre both upstream and downstream of the AVM.

### 3.5 Notch activity is not required for AVM development in *alk1* mutants

To further explore the role of enhanced Dll4/Notch in AVM development in the absence of Alk1 function, we inhibited Notch activity in *alk1* mutants and assessed cranial vascular phenotype. First, we injected a splice-blocking *dll4* morpholino<sup>4</sup> into *alk1*<sup>Y6</sup> mutants. The morpholino generated an aberrant splice product that eliminated exon 3, decreased wild-type transcript to ~37% of control, and resulted in intersegmental vessel hypersprouting<sup>4,40</sup> in 60% of embryos (Supplementary material online, Figure S4). Wild-type *dll4* morphants exhibited a small but significant increase in BCA area at 36 hpf (Figure 4A, B and I) but normal cranial vessel morphology, with no AVMs, at 48 hpf (Figure 4E, F and J). *dll4* knockdown failed to rescue increased BCA area (36 hpf) or cranial AVMs (48 hpf) in *alk1*<sup>Y6</sup> mutants (Figure 4C, D, and G–J).

Because we could not achieve complete knockdown of *dll4*, we treated *alk1* mutants with LY411575 (beginning at 23 hpf) to eliminate Notch activity and assessed cranial vascular phenotype at 36 and

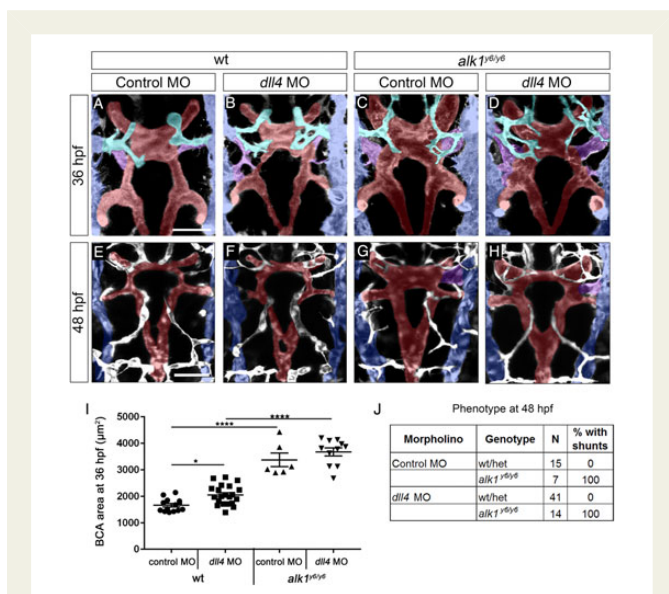


**Figure 4** *dll4* expression is not required for AVM development in *alk1* mutants. Embryos from an *alk1*<sup>Y6/+</sup>;*Tg(kdr:l:gf)*<sup>la116</sup> incross were injected at the 1–4-cell stage with 15 ng *dll4* MO or 5-bp mismatch control MO, imaged at 36 (A–D) or 48 (E–H) hpf, and genotyped. Two-dimensional projections of two-photon Z-stacks. Pseudo-colouring: PMBC (blue), CtA (cyan), CaDI/BCA/PCS/BA (red), and BCA/PMBC connection (purple). Dorsal views, anterior up. Images represent N = 7–41 embryos per condition. Scale bars, 50 µm. (I) *dll4* knockdown failed to rescue increased BCA area in *alk1*<sup>Y6</sup> mutants at 36 hpf. Lines represent mean ± SEM, N = 6–21 embryos per condition. One-way ANOVA followed by Tukey's *post-hoc* test, \**P* < 0.05; \*\*\*\**P* < 0.0001. (J) *dll4* knockdown failed to rescue cranial shunt formation in *alk1*<sup>Y6</sup> mutants at 48 hpf.

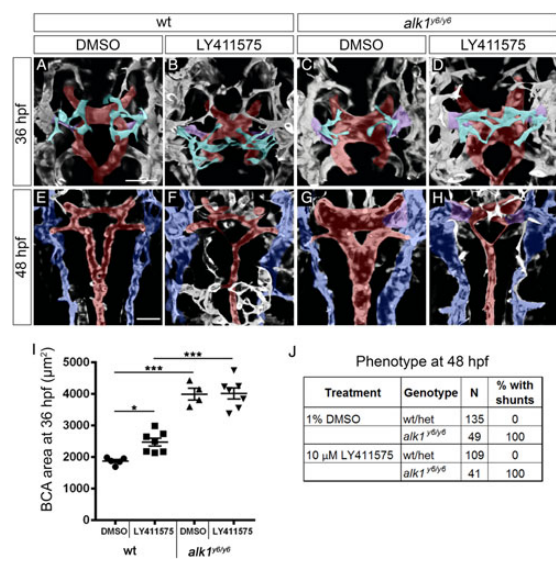


**Figure 5** Notch activity is not required for AVM development in *alk1* mutants. Embryos from an *alk1*<sup>Y6/+</sup>;*Tg(kdr:l:gf)*<sup>la116</sup> incross were treated with 1% DMSO or 10 µmol/L LY411575 at 23 hpf and cranial vasculature imaged at 36 (A–D) and 48 (E–H) hpf. Two-dimensional projections of two-photon Z-stacks; in (E–H), dorsal planes were removed to highlight BCA/PCS. Pseudo-colouring: PMBC (blue), CtA (cyan), CaDI/BCA/PCS/BA (red), and BCA/PMBC shunt (purple). Dorsal views, anterior up. Scale bars, 50 µm. (I) Notch inhibition failed to rescue increased BCA area in *alk1*<sup>Y6</sup> mutants at 36 hpf. Lines represent mean ± SEM, N = 4–7 embryos per condition. One-way ANOVA followed by Tukey's *post-hoc* test, \**P* < 0.05; \*\*\*\**P* < 0.0001. (J) Notch inhibition failed to rescue cranial shunt formation in *alk1*<sup>Y6</sup> mutants at 48 hpf.



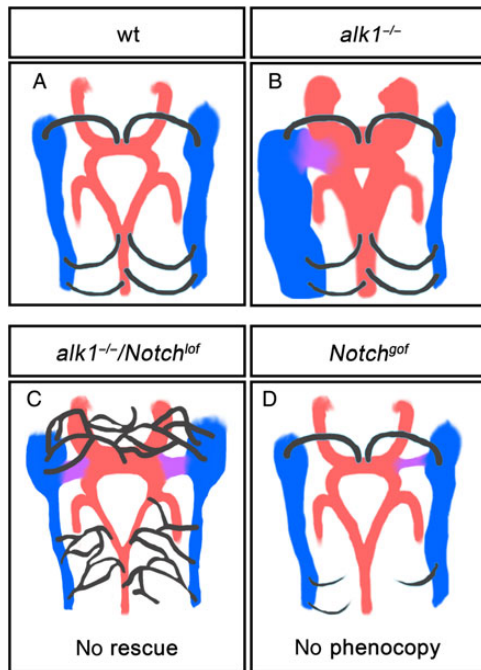


**Figure 6** Cranial vessel architecture resulting from Alk1 and/or Notch manipulation. *alk1* mutants develop enlarged cranial arteries (red) that drain through an aberrantly retained connection (purple) to major primitive drainage veins (blue). Although this phenotype is associated with increased arterial *dll4*, *notch<sup>9of</sup>* fails to phenocopy and *notch<sup>lof</sup>* fails to rescue this defect. *notch<sup>9of</sup>* causes impaired venous-derived sprouting (black), whereas *Notch<sup>lof</sup>* causes enhanced venous-derived sprouting. 48 hpf, dorsal views, anterior up.

48 hpf (Figure 5). In DMSO-treated wild-type embryos, the anterior central arteries (CtAs)<sup>49</sup> sprouted as the BCA/PMBC connection regressed: one or two sprouts emerged from more anterior aspects of each PMBC and migrated medially, with sprouts interacting ipsilaterally but not contralaterally and ultimately connecting to the BCA by 36 hpf (Figure 5A). Notch inhibition in wild-type embryos had no effect on the CaDI/BCA but caused hypersprouting in the PMBC-derived CtAs at 36 hpf, with significant increases in number of PMBC-derived sprouts, connections to the BCA, branch points, and contralateral sprout connections (Figure 5B, Supplementary material online, Figure S5A, A', B, B' and E–H).

In contrast to Notch-inhibited embryos, DMSO-treated *alk1* mutants exhibited enlarged CaDIs/BCAs at 36 hpf, as previously reported,<sup>30,31,39</sup> but PMBC-derived CtAs were unaffected (Figure 5C, Supplementary material online, Figure S5C, C', D, D' and E–H). Notch-inhibited *alk1* mutants were indistinguishable from DMSO-treated *alk1* mutants in terms of increased BCA calibre at 36 hpf (Figure 5C, D, and I). At 48 hpf, LY411575 treatment decreased PCS calibre in both wild-type and *alk1* mutant embryos but failed to rescue *alk1* mutant AVMs (Figure 5E–H and J). Furthermore, despite enhanced *dll4* expression, Notch signalling, as quantified by mean BCA EGFP fluorescence intensity in *Tg(tp1:egfp)<sup>um14</sup>* embryos, was unchanged in *alk1* morphants compared with control (Supplementary material online, Figure S6). These data support *dll4* morphant data and suggest that enhanced DLL4/Notch signalling does not underlie AVM development in the absence of *alk1*.

Although Notch inhibition failed to rescue the *alk1* mutant phenotype, *alk1* mutation dampened Notch inhibitor-induced effects on CtAs, decreasing number of PMBC-derived sprouts, number of connections to the BCA, and CtA branch points to levels between wild-type DMSO-treated and wild-type LY411575-treated embryos (Figure 5A–D, Supplementary material online, Figure S5). However, effects did not achieve statistical significance. Further studies are required to determine whether this result reflects a genetic interaction between Alk1 and Notch pathways or an effect of altered vascular haemodynamics.

## 4. Discussion

Our results in zebrafish embryos demonstrate context-specific effects of Notch signalling on arterial endothelial gene expression. Although Notch inhibition abrogated transcription of a synthetic Notch reporter and endogenous *dll4* in both trunk and cranial arteries, other arterial Notch targets were less sensitive to Notch inhibition, suggesting that additional control elements sustain expression of these genes in the absence of Notch. Furthermore, Notch sensitivity of particular genes showed regional variation, suggesting unique regulatory mechanisms in different vascular beds. These data suggest that context-specific regulation, which may be lost or dampened in cultured endothelial cells, plays an important role in the control of Notch target gene expression *in vivo*.

Based on published work demonstrating cooperative interactions between DLL4/Notch and BMP9/ALK1 in enhancing arterial Notch target gene expression in cultured endothelial cells,<sup>26</sup> we had anticipated that combined Notch and Alk1 inhibition might additively if not synergistically decrease Notch target gene expression and impair arterial specification. However, abrogation of Alk1 signalling failed to decrease expression of Notch targets or disrupt arterial (*hey2*, *efnb2a*, *dll4*) or venous (data not shown) identity, and we uncovered only minor cooperative interactions between Alk1 and Notch, with both contributing to maintenance of *efnb2a* and *hey2* expression in trunk but not cranial arteries. Furthermore, we uncovered opposing roles of Notch and Alk1 in expression of the Notch target and arterial marker, *dll4*. Although *dll4* is up-regulated in the zebrafish DA in the absence of blood flow,<sup>50</sup> lack of blood flow cannot account for increased *dll4* in *alk1* mutants: blood flow remains strong in *alk1* mutants at 36 hpf, with only a subtle redistribution of flow towards cranial vessels.<sup>31</sup> Together with previous data demonstrating increased *cxc4a* and decreased *edn1* in the absence of blood flow or *alk1* expression,<sup>31</sup> these data support the idea that Alk1 mediates a flow-based signal that controls expression of a subset of arterial genes. It is also possible that *dll4* up-regulation in the absence of *alk1* might be attributed to the loss of the Smad1/5 target, *id1*. In the DA, *id1* is down-regulated in the absence of *alk1* or blood flow (data not shown), and ID1 stabilizes HES1 (Her6 in zebrafish), which in turn represses DLL4.<sup>51,52</sup> Therefore, decreased Id1 might decrease Her6, thereby resulting in increased *dll4*. However, we were unable to detect *her6* in zebrafish arterial endothelial cells by *in situ* hybridization.

In addition to the unanticipated opposing effects of Notch and Alk1 on *dll4* expression, we demonstrated a paradoxical interaction with respect to cranial arterial *hey2* regulation, with loss of *alk1* restoring *hey2* to near control levels in Notch-inhibited embryos. This finding suggests that Alk1 may repress *hey2* in cranial arterial endothelial cells either downstream of NICD cleavage or via an independent mechanism. Although it is possible that enhanced blood flow through enlarged,



*alk1*-dependent vessels might increase *hey2* expression, this seems unlikely given that *hey2* expression is unchanged in *alk1* mutants with intact Notch signalling (Table 1) or in the absence of blood flow (data not shown).

Dll4 is a critical arterial endothelial Notch ligand<sup>5,10</sup> and Notch<sup>gof</sup> and in particular *Dll4* overexpression results in large calibre arteries and AVMs similar in morphology to AVMs in *Alk1* knockout mice.<sup>8,9,11,12,17</sup> Therefore, our finding that Alk1 inhibited *dll4* expression initially suggested to us that increased Notch signalling might contribute to AVMs in *alk1* mutants. However, multiple lines of evidence fail to support this hypothesis. First, although ectopic endothelial expression of N1ICD results in small cranial AVMs involving the same vessels as in *alk1* mutants, the origin and progression of these AVMs differs dramatically. The primary defect leading to AVMs in N1ICD-expressing embryos is delayed venous-derived sprouting, whereas the primary defect in *alk1* mutants is increased endothelial cell number in and calibre of upstream arteries.<sup>31</sup> Differences in the spatiotemporal expression of *fli1a*-driven N1ICD vs. *alk1* limit the utility of our approach; however, we would expect that earlier N1ICD expression would cause an even more pronounced arterial phenotype if enhanced arterial Notch signalling could serve as a proxy for arterial *alk1* loss. Secondly, neither *dll4* knockdown nor Notch inhibition rescues *alk1* mutant AVMs. Thirdly, despite increased *dll4* expression, we failed to detect increased canonical Notch activity in *alk1* mutants. Together, these results suggest that AVMs arise independently in Notch<sup>gof</sup> and Alk1<sup>lof</sup> embryos (Figure 6).

Although AVMs initiate via independent mechanisms in Notch<sup>gof</sup> and Alk1<sup>lof</sup> embryos, both represent retention of normally transient BCA/PMBC connections. In *alk1* mutants, maintenance of BCA/PMBC connections occurs as an adaptive response to increased shear stress caused by enlargement of upstream arteries.<sup>31</sup> In Notch<sup>gof</sup> embryos, impaired venous-derived sprouting delays CaDI/BCA drainage, which likely alters cranial vascular haemodynamics and affects remodelling. Thus, an adaptive response to altered haemodynamics, downstream of independent primary molecular and cellular defects, may be a unifying factor in the development of Notch<sup>gof</sup> and Alk1<sup>lof</sup> AVMs.

Although we failed to rescue vascular defects in *alk1* mutants via Notch inhibition, we partially rescued CtA hypersprouting defects in Notch-inhibited embryos via *alk1* mutation, suggesting some interaction between Notch and Alk1 in the cranial vasculature. It is possible that restored *hey2* expression in the absence of both Notch and Alk1 signalling might contribute to this phenomenon, as knockdown of *HEY2* enhances sprouting in cultured HUVECs.<sup>26</sup> However, whether these observations represent a true genetic interaction or a response to changes in vascular haemodynamics remains to be determined.

In summary, our *in vivo* analysis of Notch and Alk1 signalling demonstrates gene-specific and context-specific interactions, with examples of both cooperative and antagonistic control of gene expression. However, results fail to support the idea that these pathways interact synergistically to control Notch target genes, program arterial identity, and prevent AVMs.

## Supplementary material

Supplementary material is available at *Cardiovascular Research* online.

## Acknowledgements

We thank Zachary Kupchinsky for fish care; Sarah Young, Teresa Capasso, Donna Unke, and Harinee Suthakar for technical contributions; and Drs Nathan Lawson (University of Massachusetts Medical

School, Worcester, MA, USA), Brant Weinstein (NIH/NICHHD, Bethesda, MD, USA), Heinz-Georg Belting, and Markus Affolter (University of Basel, Switzerland) for reagents.

## Funding

This work was supported by the National Institutes of Health (R01 HL079108 to B.L.R.).

**Conflict of interest:** none declared.

## References

- Guruharsha KG, Kankel MW, Artavanis-Tsakonas S. The Notch signalling system: recent insights into the complexity of a conserved pathway. *Nat Rev Genet* 2012;**13**: 654–666.
- Lawson ND, Scheer N, Pham VN, Kim CH, Chitnis AB, Campos-Ortega JA, Weinstein BM. Notch signaling is required for arterial-venous differentiation during embryonic vascular development. *Development* 2001;**128**:3675–3683.
- Hellstrom M, Phng LK, Hofmann JJ, Wallgard E, Coultas L, Lindblom P, Alva J, Nilsson AK, Karlsson L, Gaiano N, Yoon K, Rossant J, Iruela-Arispe ML, Kalen M, Gerhardt H, Betsholtz C. Dll4 signalling through Notch1 regulates formation of tip cells during angiogenesis. *Nature* 2007;**445**:776–780.
- Siekman AF, Lawson ND. Notch signalling limits angiogenic cell behaviour in developing zebrafish arteries. *Nature* 2007;**445**:781–784.
- Quillien A, Moore JC, Shin M, Siekman AF, Smith T, Pan L, Moens CB, Parsons MJ, Lawson ND. Distinct Notch signaling outputs pattern the developing arterial system. *Development* 2014;**141**:1544–1552.
- Krebs LT, Shutter JR, Tanigaki K, Honjo T, Stark KL, Gridley T. Haploinsufficient lethality and formation of arteriovenous malformations in Notch pathway mutants. *Genes Dev* 2004;**18**:2469–2473.
- Duarte A, Hirashima M, Benedito R, Trindade A, Diniz P, Bekman E, Costa L, Henrique D, Rossant J. Dosage-sensitive requirement for mouse Dll4 in artery development. *Genes Dev* 2004;**18**:2474–2478.
- Carlson TR, Yan Y, Wu X, Lam MT, Tang GL, Beverly LJ, Messina LM, Capobianco AJ, Werb Z, Wang R. Endothelial expression of constitutively active Notch4 elicits reversible arteriovenous malformations in adult mice. *Proc Natl Acad Sci USA* 2005;**102**: 9884–9889.
- Krebs LT, Starling C, Chervonsky AV, Gridley T. Notch1 activation in mice causes arteriovenous malformations phenocopied by ephrinB2 and EphB4 mutants. *Genesis* 2010;**48**:146–150.
- Iso T, Maeno T, Oike Y, Yamazaki M, Doi H, Arai M, Kurabayashi M. Dll4-selective Notch signaling induces ephrinB2 gene expression in endothelial cells. *Biochem Biophys Res Commun* 2006;**341**:708–714.
- Kim YH, Hu H, Guevara-Gallardo S, Lam MT, Fong SY, Wang RA. Artery and vein size is balanced by Notch and ephrin B2/EphB4 during angiogenesis. *Development* 2008;**135**: 3755–3764.
- Trindade A, Kumar SR, Scehnet JS, Lopes-da-Costa L, Becker J, Jiang W, Liu R, Gill PS, Duarte A. Overexpression of delta-like 4 induces arterialization and attenuates vessel formation in developing mouse embryos. *Blood* 2008;**112**:1720–1729.
- Kim JH, Peacock MR, George SC, Hughes CC. BMP9 induces EphrinB2 expression in endothelial cells through an Alk1-BMPRII/ActRII-ID1/ID3-dependent pathway: implications for hereditary hemorrhagic telangiectasia type II. *Angiogenesis* 2012;**15**:497–509.
- Benedito R, Trindade A, Hirashima M, Henrique D, da Costa LL, Rossant J, Gill PS, Duarte A. Loss of Notch signalling induced by Dll4 causes arterial calibre reduction by increasing endothelial cell response to angiogenic stimuli. *BMC Dev Biol* 2008;**8**:117.
- Murphy PA, Lu G, Shiah S, Bollen AW, Wang RA. Endothelial Notch signaling is upregulated in human brain arteriovenous malformations and a mouse model of the disease. *Lab Invest* 2009;**89**:971–982.
- ZhuGe Q, Zhong M, Zheng W, Yang GY, Mao X, Xie L, Chen G, Chen Y, Lawton MT, Young WL, Greenberg DA, Jin K. Notch-1 signalling is activated in brain arteriovenous malformations in humans. *Brain* 2009;**132**:3231–3241.
- Murphy PA, Lam MT, Wu X, Kim TN, Vartanian SM, Bollen AW, Carlson TR, Wang RA. Endothelial Notch4 signaling induces hallmarks of brain arteriovenous malformations in mice. *Proc Natl Acad Sci USA* 2008;**105**:10901–10906.
- Herbert SP, Huisken J, Kim TN, Feldman ME, Houseman BT, Wang RA, Shokat KM, Stainier DY. Arterial-venous segregation by selective cell sprouting: an alternative mode of blood vessel formation. *Science* 2009;**326**:294–298.
- Lindskog H, Kim YH, Jelin EB, Kong Y, Guevara-Gallardo S, Kim TN, Wang RA. Molecular identification of venous progenitors in the dorsal aorta reveals an aortic origin for the cardinal vein in mammals. *Development* 2014;**141**:1120–1128.
- Xu P, Liu J, Derynck R. Post-translational regulation of TGF-beta receptor and Smad signaling. *FEBS Lett* 2012;**586**:1871–1884.
- Johnson DW, Berg JN, Baldwin MA, Gallione CJ, Marondel I, Yoon SJ, Stenzel TT, Speer M, Pericak-Vance MA, Diamond A, Gutmacher AE, Jackson CE, Attisano L, Kucherlapati R, Porteous ME, Marchuk DA. Mutations in the activin receptor-like

- kinase 1 gene in hereditary haemorrhagic telangiectasia type 2. *Nat Genet* 1996; **13**:189–195.
22. McDonald J, Bayrak-Toydemir P, Pyeritz RE. Hereditary hemorrhagic telangiectasia: an overview of diagnosis, management, and pathogenesis. *Genet Med* 2011; **13**:607–616.
  23. McAllister KA, Grogg KM, Johnson DW, Gallione CJ, Baldwin MA, Jackson CE, Helmbold EA, Markel DS, McKinnon WC, Murrell J, McCormick MK, Pericak-Vance MA, Heutnik P, Oostra BA, Haitjema T, Westerman CJJ, Porteous ME, Guttmacher AE, Letarte M, Marchuk DA. Endoglin, a TGF- $\beta$  binding protein of endothelial cells, is the gene for hereditary haemorrhagic telangiectasia type 1. *Nat Genet* 1994; **8**:345–351.
  24. Gallione CJ, Repetto GM, Legius E, Rustgi AK, Schelley SL, Tejpar S, Mitchell G, Drouin E, Westermann CJ, Marchuk DA. A combined syndrome of juvenile polyposis and hereditary haemorrhagic telangiectasia associated with mutations in MADH4 (SMAD4). *Lancet* 2004; **363**:852–859.
  25. Urness LD, Sorensen LK, Li DY. Arteriovenous malformations in mice lacking activin receptor-like kinase-1. *Nat Genet* 2000; **26**:328–331.
  26. Larrivee B, Prahst C, Gordon E, del Toro R, Mathivet T, Duarte A, Simons M, Eichmann A. ALK1 signaling inhibits angiogenesis by cooperating with the Notch pathway. *Dev Cell* 2012; **22**:489–500.
  27. Taylor KL, Henderson AM, Hughes CC. Notch activation during endothelial cell network formation in vitro targets the basic HLH transcription factor HESR-1 and downregulates VEGFR-2/KDR expression. *Microvasc Res* 2002; **64**:372–383.
  28. Morikawa M, Koinuma D, Tsutsumi S, Vasilaki E, Kanki Y, Heldin CH, Aburatani H, Miyazono K. CHIP-seq reveals cell type-specific binding patterns of BMP-specific Smads and a novel binding motif. *Nucleic Acids Res* 2011; **39**:8712–8727.
  29. Westerfield M. *The Zebrafish Book*. Eugene: University of Oregon Press, 1995.
  30. Roman BL, Pham VN, Lawson ND, Kulik M, Childs S, Lekven AC, Garrity DM, Moon RT, Fishman MC, Lechleider RJ, Weinstein BM. Disruption of *acvr1* increases endothelial cell number in zebrafish cranial vessels. *Development* 2002; **129**:3009–3019.
  31. Corti P, Young S, Chen CY, Patrick MJ, Rochon ER, Pekkan K, Roman BL. Interaction between *alk1* and blood flow in the development of arteriovenous malformations. *Development* 2011; **138**:1573–1582.
  32. Jin SW, Beis D, Mitchell T, Chen JN, Stainier DY. Cellular and molecular analyses of vascular tube and lumen formation in zebrafish. *Development* 2005; **132**:5199–5209.
  33. Parsons MJ, Pisharath H, Yusuff S, Moore JC, Siekmann AF, Lawson N, Leach SD. Notch-responsive cells initiate the secondary transition in larval zebrafish pancreas. *Mech Dev* 2009; **126**:898–912.
  34. Choi J, Dong L, Ahn J, Dao D, Hammerschmidt M, Chen JN. FoxH1 negatively modulates *flk1* gene expression and vascular formation in zebrafish. *Dev Biol* 2007; **304**:735–744.
  35. Scheer N, Campos-Ortega JA. Use of the Gal4-UAS technique for targeted gene expression in the zebrafish. *Mech Dev* 1999; **80**:153–158.
  36. Herwig L, Blum Y, Krudewig A, Ellertsdottir E, Lenard A, Belting HG, Affolter M. Distinct cellular mechanisms of blood vessel fusion in the zebrafish embryo. *Curr Biol* 2011; **21**:1942–1948.
  37. Traver D, Paw BH, Poss KD, Penberthy WT, Lin S, Zon LI. Transplantation and in vivo imaging of multilineage engraftment in zebrafish bloodless mutants. *Nat Immunol* 2003; **4**:1238–1246.
  38. Hatta K, Tsujii H, Omura T. Cell tracking using a photoconvertible fluorescent protein. *Nat Protoc* 2006; **1**:960–967.
  39. Laux DW, Young S, Donovan JP, Mansfield CJ, Upton PD, Roman BL. Circulating Bmp10 acts through endothelial Alk1 to mediate flow-dependent arterial quiescence. *Development* 2013; **140**:3403–3412.
  40. Leslie JD, Ariza-McNaughton L, Bermange AL, McAdow R, Johnson SL, Lewis J. Endothelial signalling by the Notch ligand Delta-like 4 restricts angiogenesis. *Development* 2007; **134**:839–844.
  41. Schulte-Merker S, Stainier DY. Out with the old, in with the new: reassessing morpholino knockdowns in light of genome editing technology. *Development* 2014; **141**:3103–3104.
  42. Borggreve T, Oswald F. The Notch signaling pathway: transcriptional regulation at Notch target genes. *Cell Mol Life Sci* 2009; **66**:1631–1646.
  43. Zhou M, Yan J, Ma Z, Zhou Y, Abbood NN, Liu J, Su L, Jia H, Guo AY. Comparative and evolutionary analysis of the HES/HEY gene family reveal exon/intron loss and teleost specific duplication events. *PLoS One* 2012; **7**:e40649.
  44. Caolo V, van den Akker NM, Verbruggen S, Donners MM, Swennen G, Schulten H, Waltenberger J, Post MJ, Molin DG. Feed-forward signaling by membrane-bound ligand receptor circuit: the case of NOTCH DELTA-like 4 ligand in endothelial cells. *J Biol Chem* 2010; **285**:40681–40689.
  45. Sacilotto N, Monteiro R, Fritzsche M, Becker PW, Sanchez-Del-Campo L, Liu K, Pinheiro P, Ratnayaka I, Davies B, Goding CR, Patient R, Bou-Gharios G, De Val S. Analysis of Dll4 regulation reveals a combinatorial role for Sox and Notch in arterial development. *Proc Natl Acad Sci USA* 2013; **110**:11893–11898.
  46. Wythe JD, Dang LT, Devine WP, Boudreau E, Artap ST, He D, Schachterle W, Stainier DY, Oettgen P, Black BL, Bruneau BG, Fish JE. ETS factors regulate Vegf-dependent arterial specification. *Dev Cell* 2013; **26**:45–58.
  47. Jiang YJ, Brand M, Heisenberg CP, Beuchle D, Furutani-Seiki M, Kelsh RN, Warga RM, Granato M, Haffter P, Hammerschmidt M, Kane DA, Mullins MC, Odenthal J, van Eeden FJ, Nusslein-Volhard C. Mutations affecting neurogenesis and brain morphology in the zebrafish, *Danio rerio*. *Development* 1996; **123**:205–216.
  48. Zhong TP, Rosenberg M, Mohideen MA, Weinstein B, Fishman MC. Gridlock, an HLH gene required for assembly of the aorta in zebrafish. *Science* 2000; **287**:1820–1824.
  49. Isogai S, Horiguchi M, Weinstein BM. The vascular anatomy of the developing zebrafish: an atlas of embryonic and early larval development. *Dev Biol* 2001; **230**:278–301.
  50. Watson O, Novodvorsky P, Gray C, Rothman AM, Lawrie A, Crossman DC, Haase A, McMahon K, Gering M, Van Eeden FJ, Chico TJ. Blood flow suppresses vascular Notch signalling via *dll4* and is required for angiogenesis in response to hypoxic signalling. *Cardiovasc Res* 2013; **100**:252–261.
  51. Moya IM, Umans L, Maas E, Pereira PN, Beets K, Francis A, Sents W, Robertson EJ, Mummery CL, Huylebroeck D, Zwijsen A. Stalk cell phenotype depends on integration of Notch and Smad1/5 signaling cascades. *Dev Cell* 2012; **22**:501–514.
  52. Bai G, Sheng N, Xie Z, Bian W, Yokota Y, Benezra R, Kageyama R, Guillemot F, Jing N. Id sustains Hes1 expression to inhibit precocious neurogenesis by releasing negative auto-regulation of Hes1. *Dev Cell* 2007; **13**:283–297.